

A Novel UWB Radar 2-D Imaging Method with a Small Number of Antennas for Simple-Shaped Targets with Arbitrary Motion

Takuya Sakamoto

Graduate School of Informatics
Kyoto University
Kyoto, 606-8501, Japan
Email: t-sakamo@i.kyoto-u.ac.jp

Yuji Matsuki

Graduate School of Informatics
Kyoto University
Kyoto, 606-8501, Japan
Email: matuki@aso.cce.i.kyoto-u.ac.jp

Toru Sato

Graduate School of Informatics
Kyoto University
Kyoto, 606-8501, Japan
Email: tsato@kuee.kyoto-u.ac.jp

Abstract—The study of UWB (Ultra Wide-Band) pulse radar has attracted great interest in a variety of applications including surveillance systems. The high-speed SEABED (Shape Estimation Algorithm based on BST and the Extraction of Directly scattered waves) imaging algorithm, is a promising candidate for the application of UWB pulse radar in fields that require real-time operation. However, since the SEABED algorithm uses signals received at multiple locations, it can only be used in systems with either array antennas or a mechanically-scanned antenna. Such systems are inevitably costly and unrealistic for applications such as surveillance. To overcome this problem, a revised SEABED algorithm was developed, which relies on the motion of the target instead of scanning an antenna. This imaging method works with only a pair of fixed antennas, even for a target with unknown shape and motion. The method cannot, however, be applied to arbitrary motion, because it assumes that the target is located on a straight line parallel to the baseline of the pair of antennas. In this paper, we extend the revised SEABED algorithm so that an accurate imaging can be achieved when applied to arbitrary target motion.

I. INTRODUCTION

Surveillance technology is indispensable in ensuring safety in our society. Although cameras are attractive for surveillance systems due to their economical cost and high resolution, there are places where camera-based systems cannot be used due to privacy considerations. This shortcoming of using cameras for surveillance can lead to a critical breach in current surveillance systems.

Using radar systems, it is possible to obtain the shape of an object without including its surface texture, thus avoiding many privacy concerns. UWB (Ultra Wide-Band) radar particularly, is a favorite tool for this purpose because of its 3-dimensional imaging capability with exceptionally high resolution. A variety of algorithms have been proposed for imaging using UWB radar systems [1], [2], [3]. However, these conventional imaging methods are based on iterative procedures, that require unrealistically intensive computation for application in surveillance systems. We have developed SEABED, a high-speed imaging algorithm [4], [5], [6], [7], to enable the use of UWB radar in areas that require real-time operations, such as surveillance. By employing a UWB

radar system in conjunction with the SEABED algorithm, 3-D images can be obtained within a short time. Hitherto, this has been difficult to achieve with conventional camera-based systems.

The SEABED algorithm relies on multiple signals observed at various locations and consequently can only be used in antenna scanning or antenna array systems. Such antenna systems are costly and unrealistic for use in applications such as surveillance systems. To avoid the use of antenna systems, a revised SEABED method [8], [9], [10] has been developed, which makes use of the motion of the target, such as a human body, instead of antenna scanning as is the case in previous works. The revised SEABED algorithm requires only a pair of fixed antennas to estimate the motion and shape of a target that moves through the radar system. However, this method cannot be applied to arbitrary motion of the target, since it assumes that the target moves in a line parallel to the antenna baseline, a condition that is critical for application in a real environment.

This paper describes a new UWB radar imaging method obtained by extending the revised conventional SEABED algorithm and which is capable of imaging targets with arbitrary motion. First, we explain the procedure of the proposed method, followed by numerical simulations that provide quantitative evidence of the performance thereof.

II. SYSTEM MODEL

For the purposes of this paper we assume that the radar antennas are installed on walls in passages as illustrated in Fig. 1. The movement of walking is considered an unknown function.

For simplicity, only 2-dimensional problems are dealt with in this paper, where the objective is to estimate the shape of a cross section of the human body. We use three omnidirectional antennas located at a particular distance X_0 , whereas the conventional model [8], [9], [10] uses only a pair of antennas. The positions of antennas #1, #2, and #3 are $(-X_0, 0)$, $(0, 0)$, and $(X_0, 0)$, respectively. The range between the scattering center and each antenna at time t is

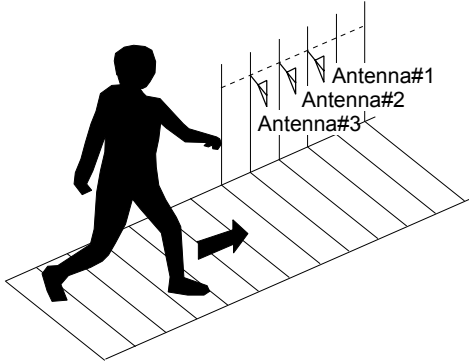


Fig. 1. Antenna arrangement in the assumed radar system.

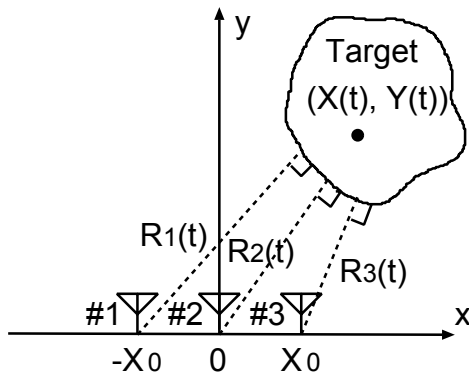


Fig. 2. 2-dimensional system model.

given as $R_1(t)$, $R_2(t)$, and $R_3(t)$ for antennas #1, #2, and #3, respectively. Let us define Δt as the IPP (Inter Pulse Period), and t_n as the n -th sampling time. Each measurement is independent of the positions of the other antennas in the system, which implies three mono-static radar systems instead of a multistatic one. The implied set of radar systems is realized by introducing a spectrum spreading modulation with three different codes assigned to the antennas. By adopting orthogonal codes, interference between antennas is reduced to zero. We assume that the target motion $\mathbf{X}(t) = (X(t), Y(t))$ is an unknown function of time t . Figure 2 depicts the 2-dimensional system model adopted in this paper.

III. CONVENTIONAL IMAGING METHOD

SEABED is a fast radar imaging algorithm developed in previous works [4], [5], [6], [7], which is applicable to the system described above only if $Y(t)$ is constant and $X(t)$ is known. The algorithm is based on a reversible transform BST (Boundary Scattering Transform) and IBST (Inverse BST) between the target shape and received signal, which requires only one of the three antennas assumed in the previous section. Here we define $R(t) = R_2(t)$, although we could equally well have used $R_1(t)$ or $R_3(t)$. With the range $R(t)$, the x -coordinate of the location of antenna $X(t)$, and the scattering center $(x(t), y(t))$ the following equations of the IBST are

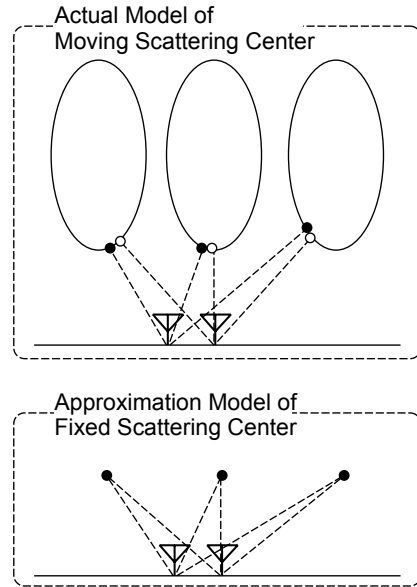


Fig. 3. Actual motion of scattering centers and an approximation with a point-line target.

satisfied as

$$\begin{cases} x(t) = -X(t) + R(t) \frac{dR(t)}{dX(t)}, \\ y(t) = R(t) \sqrt{1 - \left(\frac{dR(t)}{dX(t)}\right)^2}. \end{cases} \quad (1)$$

Because this IBST requires $X(t)$, the location of the target at time t , the SEABED algorithm cannot be used for imaging unless the movement of the target is known.

To remove the limitation of the conventional SEABED algorithm, a revised algorithm has been proposed [8], [9], [10], which employs a pair of antennas to estimate the target motion $X(t)$ under the condition $Y(t) = \text{const}$. Note that it is difficult to estimate the target location directly using a triangulation technique, because the scattering center moves along the target surface as depicted in Fig. 3. This figure shows that the motion of the scattering centers cannot be ignored for a near target of a certain size, as numerically confirmed in the previous work[10]. It is thus imperative to distinguish between the motion of the target itself and the motion of a scattering center along the surface.

For example, let the pair of antennas be $R_1(t)$ and $R_2(t)$. The revised SEABED algorithm finds a continuous function $\tau(t)$ that satisfies

$$Y_1(\tau(t)) = Y_2(t), \quad (2)$$

and then the target motion $X(t)$ is estimated as

$$X(t) \simeq \int \frac{2X_0}{\tau(t) - \tau^{-1}(t)} dt. \quad (3)$$

Now imaging can be done with the conventional SEABED algorithm using the estimated $X(t)$ in Eq. (3). Although the effectiveness of the revised SEABED algorithm has been verified [8], [9], [10], the condition $Y(t) = \text{const}$. still applies, which is not realistic in practical environments.

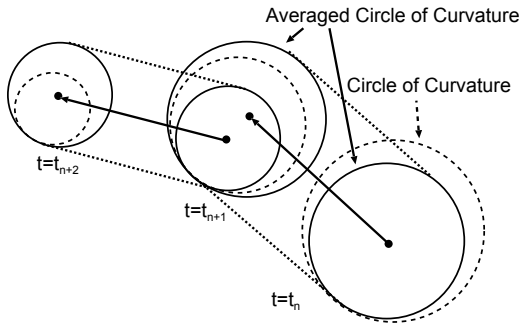


Fig. 4. Schematic of the averaging circles of curvature in the proposed method.

IV. PROPOSED IMAGING METHOD

Conventional methods enforce the unrealistic condition $Y(t) = \text{const}$. In this section, we propose a new imaging method that deals with arbitrary target motion $\mathbf{X}(t) = (X(t), Y(t))$, and uses three antennas as is the case in our system model. First, the proposed method estimates an approximate center $\mathbf{c}(t) = (c_x(t), c_y(t))$ and radius $a(t)$ of the curvature using $R_1(t)$, $R_2(t)$, and $R_3(t)$ obtained by solving

$$\begin{cases} R_1(t) = \sqrt{(c_x(t) + X_0)^2 + (c_y(t))^2} - a(t), \\ R_2(t) = \sqrt{(c_x(t))^2 + (c_y(t))^2} - a(t), \\ R_3(t) = \sqrt{(c_x(t) - X_0)^2 + (c_y(t))^2} - a(t). \end{cases} \quad (4)$$

Note that the motion of $\mathbf{c}(t)$ includes not only the target motion $\mathbf{X}(t)$, but also the relative motion of a scattering center $(x(t) - X(t), y(t) - Y(t))$ along the target surface. Therefore, $(c_x(t), c_y(t))$ cannot be used as an estimation of target motion.

To overcome this difficulty, the proposed method calculates an average radius of the curvature with $a(t_n)$ and $a(t_{n+1})$ as $\bar{a}(t_{n+\frac{1}{2}}) = (a(t_n) + a(t_{n+1})) / 2$. Then, $\mathbf{c}(t_n)$ and $\mathbf{c}(t_{n+1})$ are recalculated as $\bar{\mathbf{c}}(t_n)$ and $\bar{\mathbf{c}}(t_{n+1})$, under the condition that the radius of the curvature is equal to $\bar{a}(t_{n+\frac{1}{2}})$ when applying LMS (Least Mean Square) criteria. An instantaneous velocity vector $\mathbf{v}_{n+\frac{1}{2}}$ is defined as

$$\mathbf{v}_{n+\frac{1}{2}} = (\bar{\mathbf{c}}(t_{n+1}) - \bar{\mathbf{c}}(t_n)) / \Delta t. \quad (5)$$

This operation effectively separates the target motion $\mathbf{X}(t)$ from the relative motion of a scattering center $(x(t) - X(t), y(t) - Y(t))$ since the motion of a scattering center dominates the effect on the radius of the curvature $a(t)$. In addition, the radius of the curvature $a(t)$, in conjunction with the target motion $\mathbf{X}(t)$, have a great effect on the center of the curvature $\mathbf{c}(t)$. This procedure is illustrated graphically in Fig. 4, in which the three circles of curvature at $t = t_n, t_{n+1}, t_{n+2}$ are depicted with dashed lines. The averaged circles of curvature using adjacent pairs $t = t_n, t_{n+1}$ and t_{n+1}, t_{n+2} are shown as solid lines. Each velocity vector is represented by an arrow from the center of one averaged circle to another.

Finally, we combine the instantaneous velocity vector with

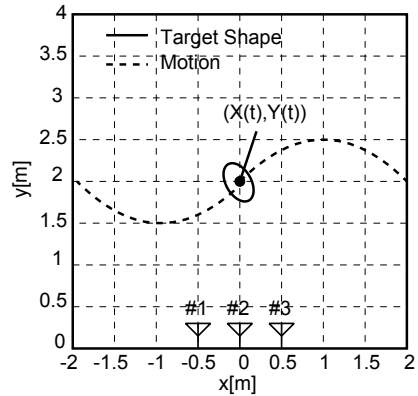


Fig. 5. Assumed system model for the numerical simulation.

a summation in the form

$$\bar{\mathbf{X}}(t_{N+\frac{1}{2}}) = \sum_{n=1}^N \mathbf{v}_{n+\frac{1}{2}} \Delta t \quad (6)$$

to obtain the estimation of the target location $\bar{\mathbf{X}}(t)$. Note that the initial value $\mathbf{X}(0)$ does not have any effect on the imaging results because it affects only the location of the estimated image. Using this estimated target motion $\bar{\mathbf{X}}(t)$, SEABED can now be applied to realize imaging even in the case of arbitrary target motion.

V. PERFORMANCE EVALUATION OF THE PROPOSED METHOD

In this section, we validate the performance of the proposed imaging method by means of numerical simulations. The assumed calculation parameters for the simulations are described below. The target shape is assumed to be a slant ellipse with a major axis of 0.25m and minor axis of 0.15m as in Fig. 5. This represents an approximated size of a section of the human body. The antenna interval is $X_0 = 0.5\text{m}$, while the assumed IPP $\Delta t = 5\text{msec}$. Target motion is given as $(X(t), Y(t)) = (v_x t, y_0 + y_f \sin \omega t)$, where $v_x = -1.0\text{m/sec}$, $y_0 = 2.0\text{m}$, $y_f = 0.5\text{m}$ and $\omega = 1.0\text{rad/sec}$. This motion model is used to investigate the performance of the imaging method in the worst case scenario. The typical walking motion of a human is obviously more likely to be in a straight line. Data obtained under these conditions for $-2\text{sec} \leq t \leq 2\text{sec}$ is shown in Fig. 6. For simplicity, we assume ideal conditions without noise.

Figure 7 shows the estimated target motion produced by the proposed algorithm. The actual and estimated motion curves overlap almost entirely, indicating that the accuracy of the estimation is quite high. Figure 8 shows the target shape estimated using the proposed algorithm. The RMS (Root Mean Square) error of the shape estimation is about 4.0 mm, which corresponds to 1.6% of the major axis and 2.7% of the minor axis of the assumed target shape.

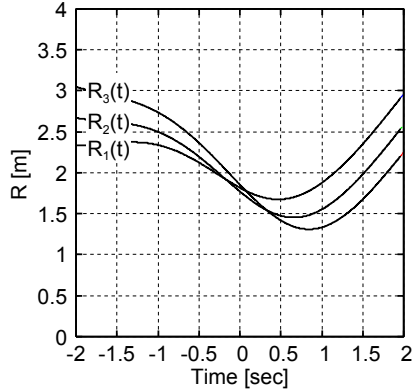


Fig. 6. Received data $R_1(t)$, $R_2(t)$ and $R_3(t)$.

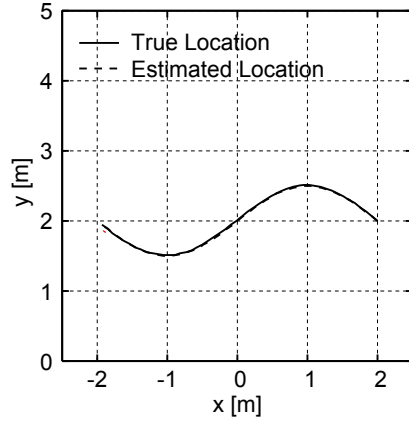


Fig. 7. Target motion estimated using the proposed method.

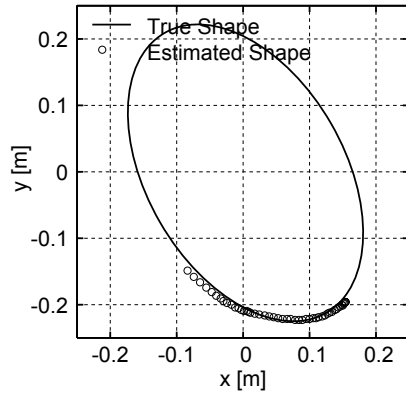


Fig. 8. Target shape estimated using the proposed method.

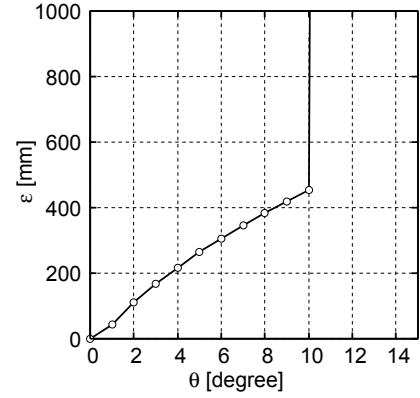


Fig. 9. RMS error of the revised conventional SEABED algorithm with an inclination angle θ for target motion along a straight line.

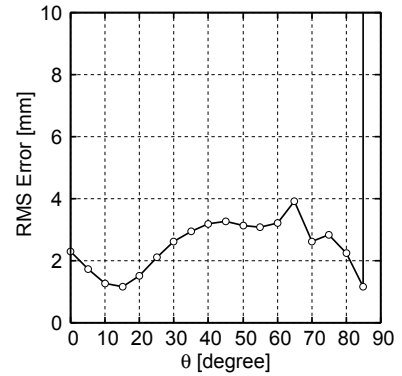


Fig. 10. RMS error of the proposed method with an inclination angle θ for target motion along a straight line.

VI. PERFORMANCE COMPARISON WITH THE CONVENTIONAL METHOD

Next, we verify the performance limitation of the revised conventional SEABED algorithm [10] with respect to target motion that does not satisfy the condition $Y(t) \neq \text{const}$. For simplicity, we assume uniform motion along a straight line with an inclination angle θ to the antenna baseline. The RMS error of the shape estimation using the revised conventional SEABED algorithm is shown in Fig. 9. Here, the target shape is the same as in Fig. 5. The assumed model for the revised SEABED algorithm corresponds to $\theta = 0^\circ$, where the RMS error is sufficiently small, thereby indicating that an accurate imaging can be realized. The RMS error, however, is relatively large even for $0^\circ < \theta \leq 10^\circ$, proving that this method does not work at all for $\theta > 10^\circ$.

In contrast, the RMS error of the shape estimation using the proposed method under the same conditions is shown in Fig. 10. This result confirms that the proposed method is able to estimate the target shape accurately for any angle except $\theta \simeq 90^\circ$.

VII. DISCUSSION

First, we clarify why three antennas are necessary for the proposed method. If only two antennas #1 and #2 were

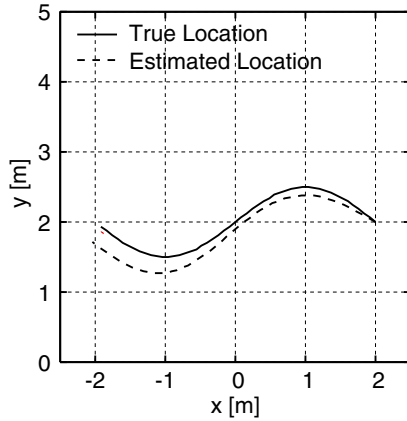


Fig. 11. Locus of the center of curvature.

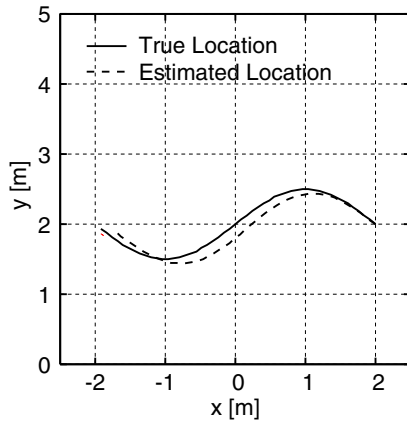


Fig. 12. Locus of the estimated scattering center.

used, all the observed data would be either $R_1(t)$ or $R_2(t)$. In general, the locations of the scattering centers for these antennas are different, as illustrated in Fig. 3. However, when a point-like target is assumed, the location can be uniquely determined with $R_1(t)$ and $R_2(t)$ and the antenna interval X_0 using a triangulation technique. In other words, these two cases cannot be distinguished if only two antennas are used. Therefore, the use of three antennas is a necessary condition for imaging a target with arbitrary motion. In this paper, we showed that our proposed method can estimate arbitrary motion with three antennas. This implies that the use of three antennas is a sufficient condition for this problem.

Next, we discuss the reason why the averaging of two radii is necessary. One might assume that the center of curvature or the estimated scattering center could be used as an estimation of target motion $\mathbf{X}(t)$. In fact, neither of these values can be used for this estimation. Figures 11 and 12 show the loci of the center of curvature $c(t)$ and the scattering center estimated by assuming a point-like target. The assumed model is the same as in the previous section. Both the results show that such simple methods cannot be used to estimate target motion, since these methods are not able to separate the motion of the target from the motion of a scattering center.

As for the distance X_0 between antennas, note that X_0 is approximately equivalent to the baseline in an interferometry technique, which means that a larger X_0 gives a more accurate estimation of angles. However, the proposed method assumes that the three antenna elements are located close together, because the curvature is approximately estimated under this condition. After considering both of these factors, we have empirically chosen $X_0 = 0.5\text{m}$.

VIII. CONCLUSION

In this paper we have discussed an imaging method for UWB (Ultra Wide-Band) pulse radar systems, particularly for application in surveillance systems. The revised conventional SEABED algorithm is a fast real-time UWB radar imaging method that employs a pair of fixed antennas and is able to estimate target shapes even for unknown target motion. However, this method requires that the motion is parallel to the antenna baseline, which is impractical in real environments. To overcome this problem, we proposed a new UWB radar imaging method. Although this method requires an additional antenna, using three antennas in total, it provides an accurate estimation of target motion and shapes for arbitrary motion without any conditions. The performance of the proposed method has thus far been verified only with numerical simulations. An experimental investigation of its performance is an important future task.

REFERENCES

- [1] E. J. Bond, X. Li, S. C. Hagness, and B. D. van Veen, "Microwave imaging via space-time beamforming for early detection of breast cancer," *IEEE Trans. Antennas Propagat.*, vol. 51, no. 8, pp. 1690–1705, 2003.
- [2] J. van der Kruk, C. P. A. Wapenaar, J. T. Fokkema, and P. M. van den Berg, "Three-dimensional imaging of multicomponent ground-penetrating radar data," *Geophysics*, vol. 68, no. 4, pp. 1241–1254, 2003.
- [3] T. Sato, T. Wakayama, and K. Takemura, "An imaging algorithm of objects embedded in a glossy dispersive medium for subsurface radar data processing," *IEEE Trans. Geosci. Remote Sensing*, vol. 38, no. 1, pp. 296–303, 2000.
- [4] T. Sakamoto and T. Sato, "A target shape estimation algorithm for pulse radar systems based on boundary scattering transform," *IEICE Trans. Commun.*, Vol. E87-B, No. 5, pp. 1357–1365, May, 2004.
- [5] T. Sakamoto and T. Sato, "A phase compensation algorithm for high-resolution pulse radar systems," *IEICE Trans. Communications*, vol. E87-B, no. 11, pp. 3314–3321, Nov., 2004.
- [6] T. Sakamoto, "A 2-D image stabilization algorithm for UWB pulse radars with fractional boundary scattering transform," *IEICE Trans. on Commun.* vol. E90-B, no. 1, pp. 131–139, Jan., 2007.
- [7] T. Sakamoto, "A fast algorithm for 3-dimensional imaging with UWB pulse radar systems," *IEICE Trans. on Commun.*, vol. E90-B, no. 3, p. 636–644, Mar. 2007.
- [8] T. Sakamoto, and T. Sato, "Real-time imaging of human bodies with UWB radars using walking motion," 2007 IEEE International Conference on Ultra-WideBand (ICUWB2007), Sep. 2007.
- [9] T. Sakamoto, and T. Sato, "A Study on Fast Imaging for Walking Human Bodies by UWB Radar with Realistic Motion Model," 2008 IEEE International Conference on Ultra-WideBand (ICUWB2008), Sep. 2008.
- [10] T. Sakamoto and T. Sato, "2-Dimensional Imaging for Human Bodies with UWB Radar using Approximately Uniform Walking Motion along a Straight Line with the SEABED Algorithm," *IEICE Trans. on Commun.*, vol. E91-B, no. 11, pp. 3695–3703, Nov. 2008.